APPLIED AND ENVIRONMENTAL MICROBIOLOGY, Jan. 1991, p. 138–145
0099-2240/91/010138-08$02.00/0

Vol. 57, No. 1

Temperature Effects on Bacterial Leaching of Sulfide Minerals in Shake Flask Experiments

LASSE AHONEN[1]† AND OLLI H. TUOVINEN[2]*

Department of Microbiology, University of Helsinki, SF-00710 Helsinki, Finland,[1] and Department of Microbiology, The Ohio State University, 484 West 12th Avenue, Columbus, Ohio 43210-1292[2]

Received 10 October 1990/Accepted 16 October 1990

The microbiological leaching of a sulfide ore sample was investigated in shake flask experiments. The ore sample contained pyrite, pyrrhotite, pentlandite, sphalerite, and chalcopyrite as the main sulfide minerals. The tests were performed at eight different temperatures in the range of 4 to 37°C. The primary data were used for rate constant calculations, based on kinetic equations underlying two simplified models of leaching, i.e., a shrinking particle model and a shrinking core model. The rate constants thus derived were further used for the calculation of activation energy values for some of the sulfide minerals present in the ore sample. The chalcopyrite leaching rates were strongly influenced by the interaction of temperature, pH, and redox potential. Sphalerite leaching could be explained with the shrinking particle model. The data on pyrrhotite leaching displayed good fit with the shrinking core model. Pyrite leaching was found to agree with the shrinking particle model. Activation energies calculated from the rate of constants suggested that the rate-limiting steps were different for the sulfide minerals examined; they could be attributed to a chemical or biochemical reaction rather than to diffusion control.

Current commercial-scale operations involving biological oxidation and solubilization of copper and uranium ores are carried out at ambient temperatures. In dumps, heaps, underground stopes, or in situ processes, the prevailing temperatures may display extremes such as those found under snow cover or in elevated temperature zones. While efforts in bench and pilot studies involve incubation temperatures which are near optimum for bacterial growth and activities, temperature control measures for leach liquors are not practiced in leach mines. Temperature profiles in underground mines display wide variation depending on the depth and geology of the formation. Temperatures of <10°C are not uncommon and they show little seasonal pattern. Temperature-related differences between leach mine operations and bench studies make it difficult to utilize laboratory data to evaluate large-scale biological leaching processes.

We have previously determined temperature-related effects on bacterial enrichment and growth with ferrous iron and elemental sulfur in the range of 4 to 37°C (1, 2). For the present work we have utilized sulfide ore samples as energy substrates for bacterial enrichment studies at suboptimal and near-optimal temperatures. Differences between ambient temperatures in leach mines and near-optimum temperature conditions in laboratory studies prompted us to determine bacterial leaching rates at suboptimal temperatures. In the present paper, the results from shake flask leaching experiments are reported. These experiments were undertaken to describe temperature effects on the kinetics of the bacterial leaching of chalcopyrite (general formula, $CuFeS_2$), sphalerite (ZnS), Co,Ni-pentlandite ($[Co,Ni]_8S_9$), pyrrhotite ($Fe_{1-x}S$), and pyrite (FeS_2) present in the ore sample.

The evaluation of rate constants requires the determination of suitable kinetic equations. Two basic models were evaluated for this purpose. First, a shrinking particle model was tested which assumes that the leaching rate is directly proportional to the surface area of the mineral. Because continuous measurement of the surface area during the experiment was not possible, the model was further simplified by replacing the surface area with the residual mass of the mineral. This treatment makes the model formally analogous with the first-order homogeneous reaction. Second, a simplified shrinking core model was tested which assumes that the rate is inversely proportional to the extent of the dissolution process and thus to the concentration of the dissolved metal. This phenomenon can be due to the formation of the product zone. A similar kinetic effect also follows when the leach liquor has to penetrate an increasing distance inside the particle before it reaches the contact surface.

MATERIALS AND METHODS

The initial source of the inoculum was a composite water sample collected from a copper mine (1). Both static and shake flask culture conditions were used in the initial enrichment. Enrichment experiments under static culture conditions were carried out at 4, 7, 10, 13, 16, 19, 28, 37, and 46°C (±1°C). Shake flask enrichment cultures were incubated at 7, 16, 28, and 37°C. All cultures were prepared in mineral salts media which contained 0.4 g each of $(NH_4)_2SO_4$, K_2HPO_4, and $MgSO_4 \cdot 7H_2O$ (pH 2.5) per liter. Media containing 10% (wt/vol) sulfide ore material were inoculated with the composite mine water sample and incubated in shaking (180 rpm) or static 250-ml flasks at each test temperature.

Once established, the cultures were tested in shake flask leaching experiments. Duplicate flasks were used for each test temperature, and control (uninoculated) flasks were also used to estimate the chemical leaching rates. Some cultures were also tested at temperatures other than that used for original enrichments.

The sulfide ore material was ground to a −590-μm size fraction for the leaching experiments. Partial elemental analysis of the ore sample indicated the following elemental composition (wt/wt): total S, 38.2%; Cu, 6.01%; Ni, 0.076%;

* Corresponding author.
† Present address: Geological Survey of Finland, SF-02150 Espoo, Finland.

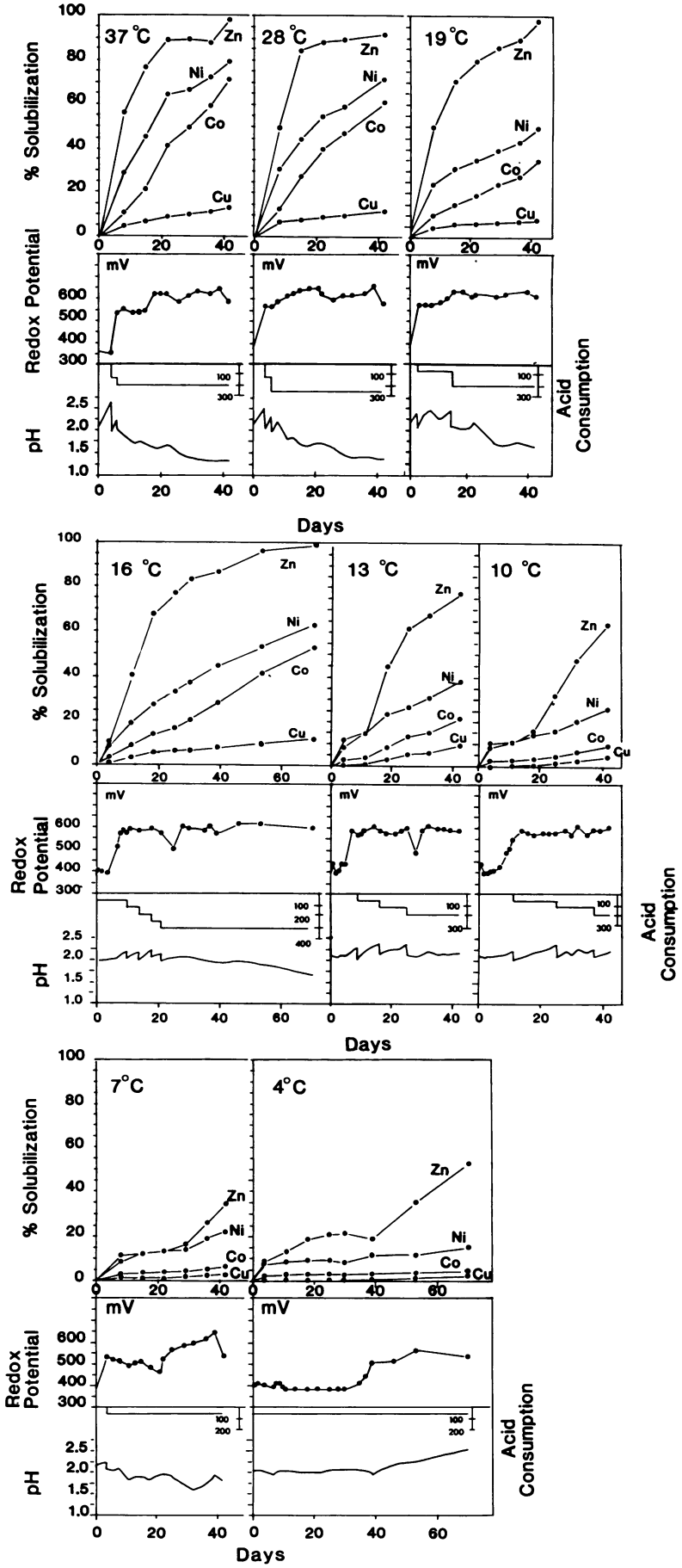

FIG. 1. Leaching of sulfide ore material at the test temperatures.

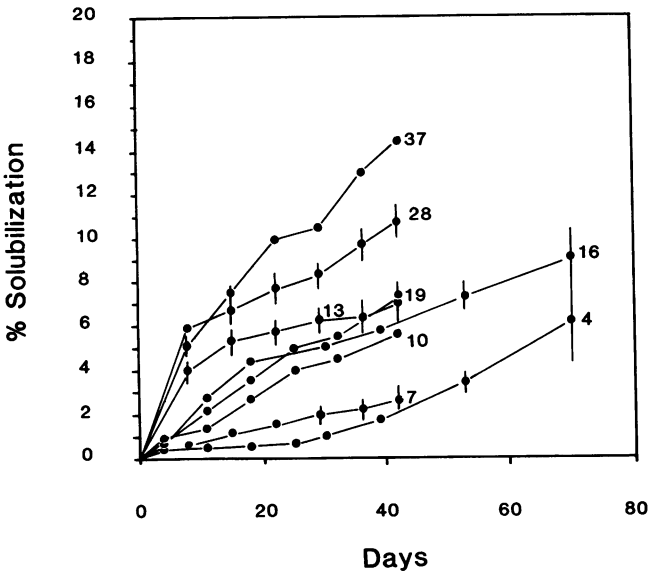

FIG. 2. Leaching of copper from chalcopyrite at each test temperature. Bars indicate standard error.

Co, 0.45%; Fe, 40.4%; and SiO_2, 17.3. Based on the chemical analysis and on mineralogical examination, the ore sample was estimated to contain approximately 17% chalcopyrite, 0.7% sphalerite, 0.4% Co,Ni-pentlandite (Co-Ni, ~1:1), 40% pyrite, and 20% pyrrhotite. Pyrite contained 0.6% Co and 0.02% Ni. Pyrrhotite contained 0.03% Co and 0.3% Ni. Pentlandite contained 23% Co and 23% Ni. Quartz was the main gangue mineral, in association with silicates and oxides. The bulk ore sample was characterized by a relatively low acid consumption, indicating the relative absence of alkaline ore materials.

The leaching of the sulfide ore material was monitored by the determination of pH, redox potential, and soluble copper, nickel, zinc, and cobalt. In initial phases it was necessary to add sulfuric acid because of the acid-consuming characteristic of the ore, but during active leaching periods the reactions were acid producing. Redox potential was measured with a Pt electrode; a standard calomel electrode

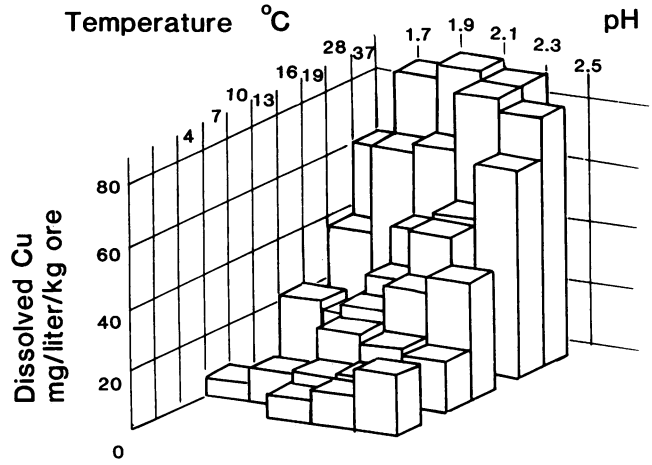

FIG. 3. Temperature and pH relationship in the bacterial leaching of chalcopyrite.

TABLE 1. Kinetic parameters of copper leaching from chalcopyrite

Temp (°C)	Rate constant, k (1/day)	Rate (dy/dt) (%/day)	$t_{1/2}$ (days)
37	0.0049	0.49	142
28	0.0042	0.42	164
19	0.0026	0.26	266
16	0.0021	0.21	329
13	0.0017	0.17	415
10	0.0011	0.11	624
7	0.0007	0.07	1,050
4	0.0005	0.05	1,390

(SCE) was used as a reference. Redox potential values (SCE scale) were initially below 400 mV and increased to the 550- to 600-mV range when active leaching started. At low temperatures this increase was gradual, taking several weeks, whereas at high temperatures the redox potential increased within a few days. Dissolved metals (Cu, Co, Ni, and Zn) were analyzed by atomic absorption spectrometry.

The kinetic models were evaluated with experimentally determined values of k which were calculated from the metal release data. These rate constants were determined as slopes of linear lines which were calculated by the method of the sum of the least squares. The k values are strictly valid only within each set of experiments, and a comparison of k values for different sets of results or different metals cannot be made based on the results in the present work.

The equations were based on a shrinking particle model and a shrinking core model. The theoretical as well as experimental bases of these models have been presented previously (3, 5, 6).

The rate equation for the shrinking particle model is

$$dy/dt = k \cdot (W_0 - y) \quad (1)$$

from which the rate constant (k) was solved

$$k = \frac{\ln [W_0/W_0 - y]}{t} \quad (2)$$

where W_0 is the initial concentration of the metal in the ore material, y is the extent of the dissolution process expressed as the concentration of the dissolved metal, and t is the time (days).

The rate equation for the shrinking core model is

$$dy/dt = k'/y \quad (3)$$

from which the rate constant was solved

$$k = y/\sqrt{t} \quad (4)$$

where $k = \sqrt{2k'}$. Thus, there is a parabolic relationship between y and t.

The half-lives of mineral dissolution ($t_{1/2}$) were determined from the respective rate constants as $\ln 2/k$.

The rate constants were further used for estimation of the activation energy (E_a) values:

$$\ln k = \ln A - E_a/RT \quad (5)$$

where A is the Arrhenius constant, R is the universal gas constant, and T is the temperature in kelvin. For a plot of $\ln k$ versus $1/T$, the slope is equal to E_a/R. The E_a values were calculated from the linear part of the Arrhenius diagrams.

RESULTS

Leaching experiments. The primary leaching data determined as changes in metal concentrations, redox potential,

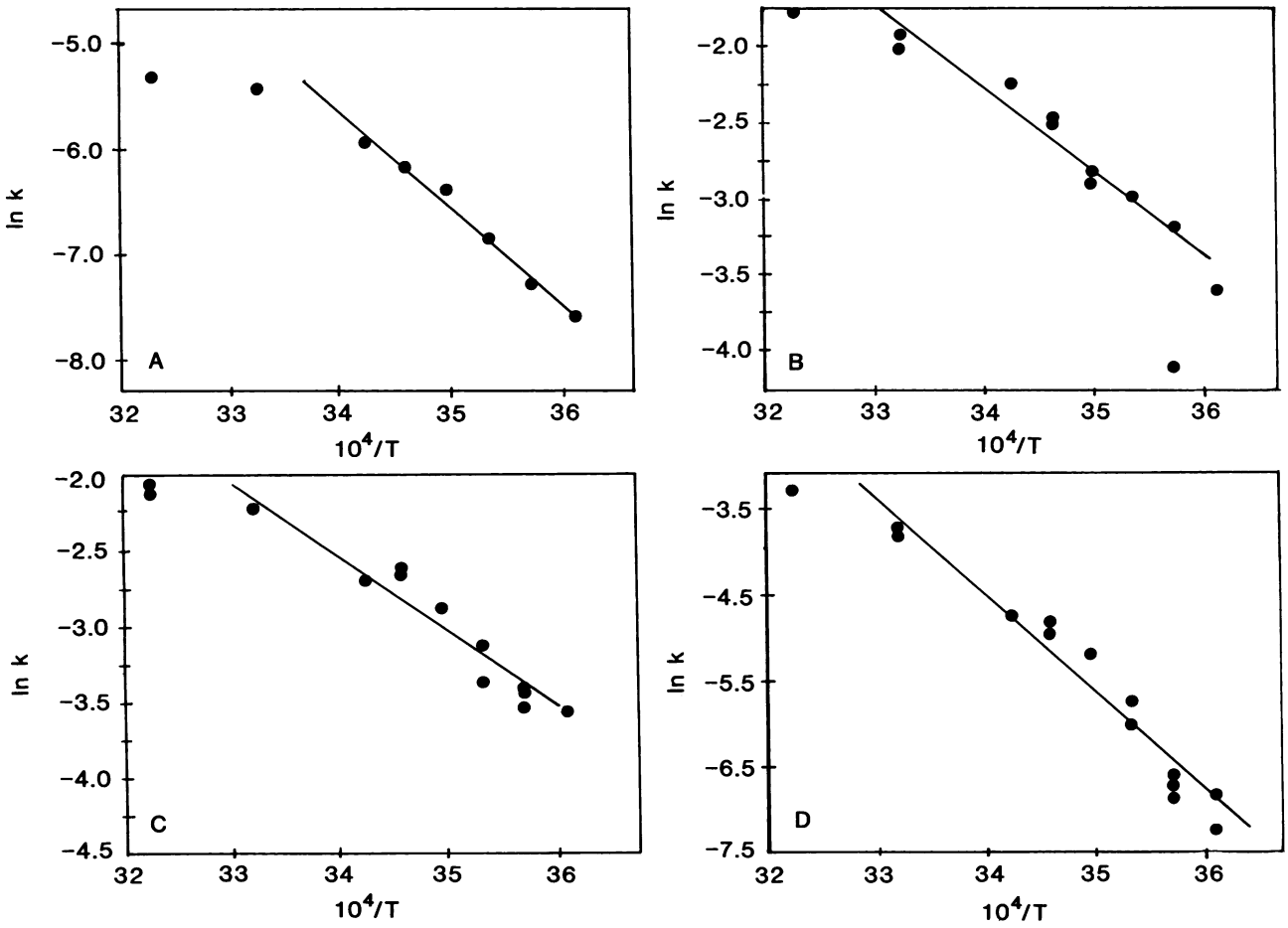

FIG. 4. Arrhenius plot of rate constants for the bacterial leaching of (A) chalcopyrite, (B) sphalerite, (C) pyrrhotite, and (D) pyrite.

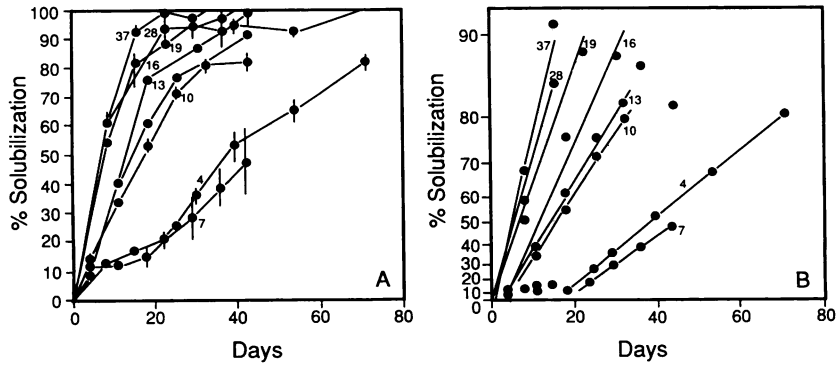

FIG. 5. Leaching of zinc from sphalerite (A) and linearized plot of zinc leaching (B) at each test temperature, based on the shrinking particle model.

TABLE 2. Kinetic parameters of zinc leaching from sphalerite

Temp (°C)[a]	Rate constant, k (1/day)	Correlation coefficient	Rate (dy/dt) (%/day)	$t_{1/2}$ (days)
37A	0.1600	0.983	16.0	4.3
28A	0.0914	0.997	9.1	7.6
28B	0.1250	0.996	12.5	5.5
28C	0.1340	0.998	13.5	5.2
19A	0.1050	0.979	10.5	6.6
16A	0.0819	0.985	8.2	8.5
16B	0.0838	0.969	8.4	8.3
13A	0.0592	0.998	5.9	11.7
13B	0.0551	0.986	5.5	12.6
10A	0.0503	0.979	5.0	13.8
10B	0.0503	0.999	5.0	13.8
7A	0.0161	0.983	1.6	43.0
7B	0.0167	0.998	1.7	41.5
7D	0.0411	0.996	4.1	16.9
4A	0.0270	0.995	2.7	25.7
4B	0.0236	0.999	2.4	29.4

[a] Letter designations indicate source of the inoculum: A, the inoculum culture was grown at the same temperature as used for the subculture; B, the inoculum was previously grown at 19°C; C, the inoculum was previously grown at 7°C; D, the inoculum was previously grown at 28°C.

TABLE 3. Kinetic parameters of nickel dissolution, representing the leaching of pyrrhotite, and estimated time courses ($t = y^2/k^2$) to reach 25, 50, and 90% dissolution of pyrrhotite ($t_{25\%}$, $t_{50\%}$, and $t_{90\%}$)

Temp (°C)[a]	Rate constant, k (1/day)	Correlation coefficient	Calculated leaching times (days)		
			$t_{25\%}$	$t_{50\%}$	$t_{90\%}$
37A	0.1340	0.987	3.5	14	45
37B	0.1250	0.990	4.0	16	52
28A	0.1220	0.996	4.2	17	55
28B	0.1120	0.998	5.0	20	65
28C	0.1110	0.995	5.1	20	66
19A	0.0709	0.992	13	50	160
16A	0.0738	0.991	12	46	150
16B	0.0777	0.991	10	41	130
13A	0.0594	0.999	18	71	230
13B	0.0586	0.988	18	73	240
10A	0.0460	0.982	30	120	380
10B	0.0361	0.966	48	190	620
7A	0.0337	0.980	55	220	710
7B	0.0222	0.976	130	500	1,600
7D	0.0347	0.982	52	210	670
4A	0.0298	0.974	70	280	910
4B	0.0143	0.928	310	1,200	3,900

[a] Letter designations indicate source of the inoculum: A, the inoculum culture was grown at the same temperature as used for the subculture; B, the inoculum was previously grown at 19°C; C, the inoculum was previously grown at 7°C; D, the inoculum was previously grown at 28°C.

and pH values as well as acid consumption are summarized in Fig. 1 for each test temperature. Of the metals of interest associated with the sulfide minerals in the ore material, zinc was leached most quantitatively. After 6 weeks, the yields of sphalerite solubilization were 90 to 100% at 16, 19, 28, and 37°C. Within this same temperature range, soluble nickel reached 50 to 70% recovery, representing the leaching of sulfide minerals pyrrhotite, pentlandite, and pyrite. The relative recalcitrance of chalcopyrite to chemical and microbiological leaching was evidenced by low concentrations of soluble copper at all test temperatures, amounting to <15% dissolution of this mineral. At the lower range of test temperatures, the leaching yields declined and the apparent leaching rates for each metal analyzed also appeared to decrease as the temperature was lowered.

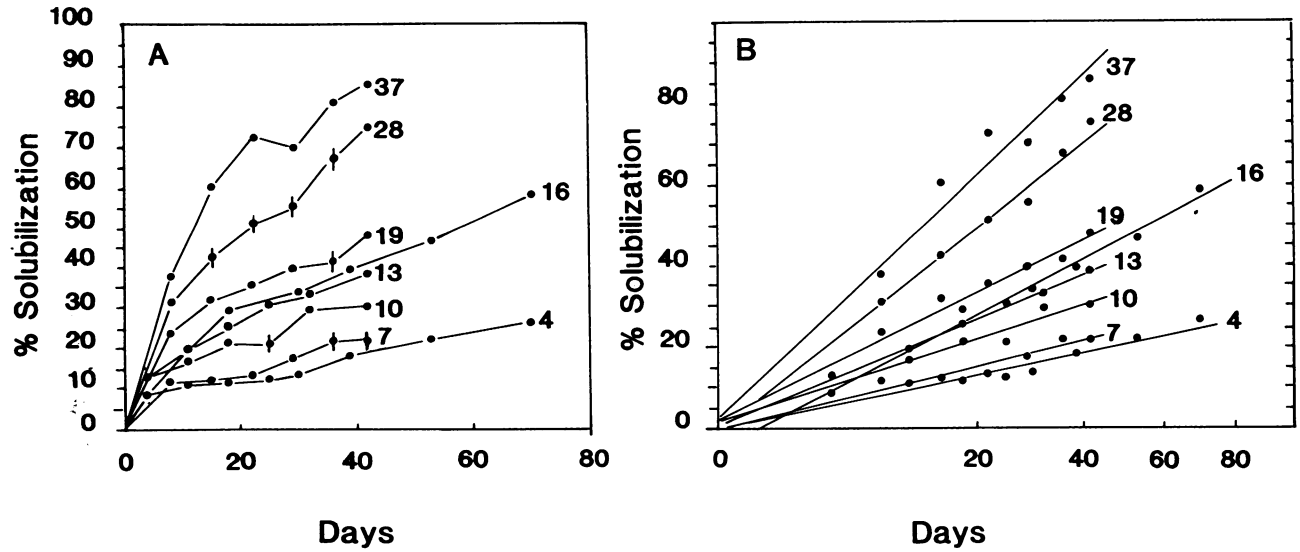

FIG. 6. Leaching of nickel (A) and linearized plot of nickel leaching (B) at each test temperature, based on the shrinking core model.

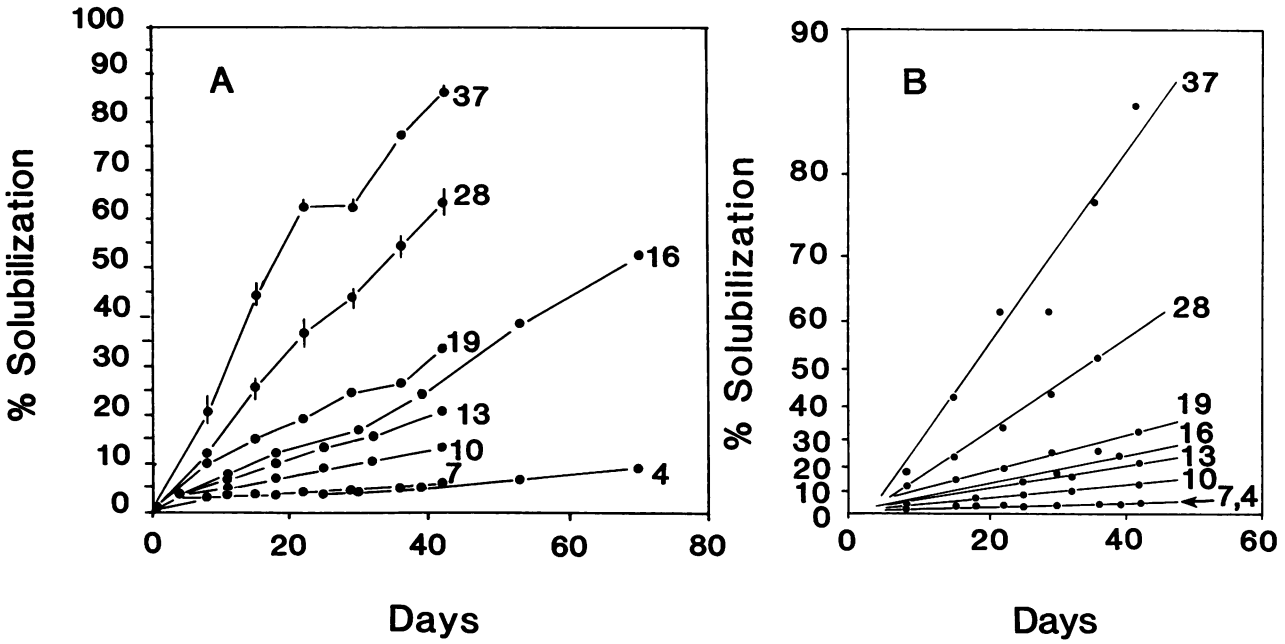

FIG. 7. Leaching of cobalt (A) and linearized plot of pyrite leaching (B) based on dissolved cobalt concentrations and the shrinking particle model.

It can also be seen in Fig. 1 that there were considerable changes in pH and redox potential values, relating to the temperature of incubation. At the higher range of test temperatures, the ore sample displayed acid-producing characteristics. The decreases in the pH can be related, by and large, to sulfuric acid production due to the bacterial oxidation of sulfide entities in the minerals. The respective redox potential values at around 600 mV (SCE) displayed oxidizing conditions. These values are comparable to those where the redox potential is determined by Fe^{3+}/Fe^{2+}. In the present work, pyrrhotite and pyrite were the two major iron sulfides in addition to a minor source of iron in the form of chalcopyrite. At the lower test temperatures, net acid consumption prevailed because of the lack of bacterial oxidation of sulfide minerals. The redox potential values either remained at a lower level or displayed a prolonged lag period before increasing to around 600 mV (SCE). All of these changes

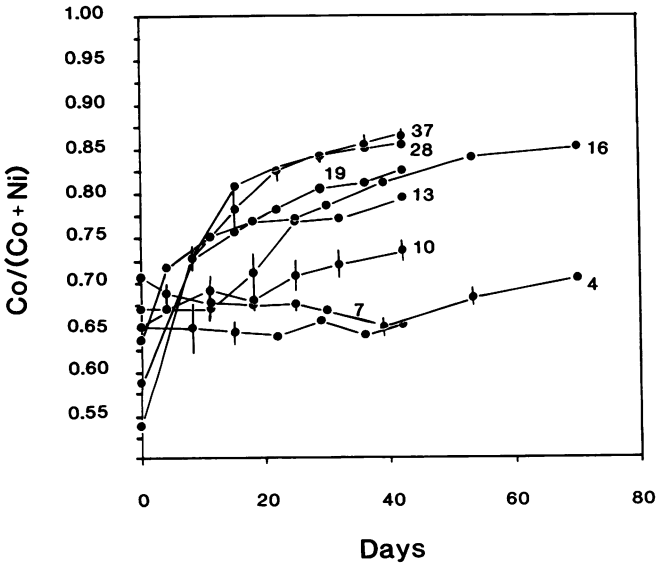

FIG. 8. Molar ratio of cobalt and nickel [Co/(Co + Ni)] during leaching.

TABLE 4. Kinetic parameters of cobalt dissolution, representing the leaching of pyrite and pentlandite

Temp (°C)[a]	Rate constant, k (1/day)	Correlation coefficient	Rate (%/day)	$t_{1/2}$ (days)
37A	0.0445	0.982	4.54	15.6
37B	0.0370	0.977	3.77	18.7
28A	0.0220	0.993	2.22	31.5
28B	0.0240	0.993	2.42	28.9
28C	0.0224	0.988	2.27	30.9
19A	0.00880	0.987	0.88	78.8
16A	0.00690	0.996	0.69	100
16B	0.00823	0.994	0.83	84.5
13A	0.00566	0.998	0.57	121
13B	0.00563	0.988	0.57	124
10A	0.00321	0.989	0.32	217
10B	0.00255	0.975	0.26	267
7A	0.00109	0.922	0.11	630
7B	0.00124	0.942	0.12	578
7D	0.00134	0.939	0.13	533
4A	0.00109	0.951	0.11	630
4B	0.00071	0.839	0.07	980

[a] Letter designations indicate source of the inoculum: A, the inoculum culture was grown at the same temperature as used for the subculture; B, the inoculum was previously grown at 19°C; C, the inoculum was previously grown at 7°C; D, the inoculum was previously grown at 28°C.

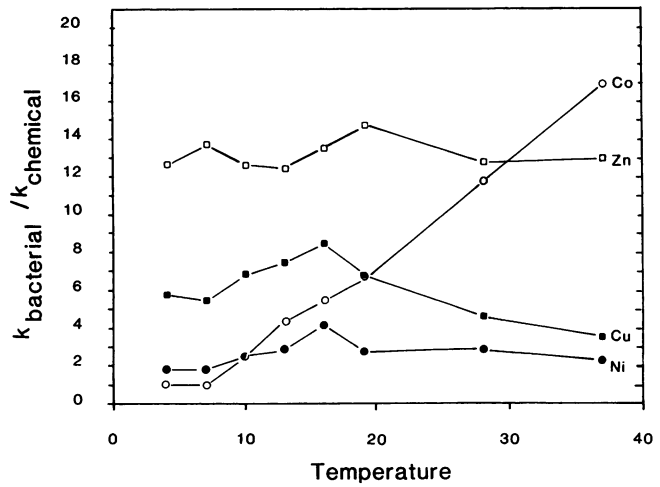

FIG. 9. Ratios of experimentally determined rate constants for bacterial and chemical leaching ($k_{bacterial}/k_{chemical}$) at the test temperature.

indicated a slower bacterial activity at the lower temperature range.

Leaching of chalcopyrite. To quantitate the temperature-dependent responses, the leaching rates were calculated separately for each metal. These data were then taken to represent the leaching of the major sulfide minerals. The solubilization of copper at each test temperature is shown in Fig. 2. Figure 2 shows the solubilization of copper at each test temperature. The leaching at the higher temperature range was initially fast and subsequently declined to slower rates. At the lower temperature range the rates were initially slow and subsequently increased to faster rates, which appeared to remain constant. The initially slow rates at the lower temperature range can be attributed to the lag phases preceding active bacterial leaching. These lag phases were also apparent from the slow increase in the redox potential at low test temperatures.

The solubilization of copper from chalcopyrite was found to be dependent on several factors in addition to the temperature. Of these, especially the redox potential and pH were important. No effort was made to characterize these dynamic interactions by statistical analysis. An example of these interactive relationships in the redox potential range of >550 mV is shown in Fig. 3.

The change in the mass of chalcopyrite during the dissolution was taken to be negligible, and thus the leaching rates were also used as the respective rate constants. The k values in the pH range 2.1 to 2.5 displayed the most pronounced temperature dependence and were selected for the estimation of the activation energy. The kinetic parameters of copper leaching are presented in Table 1. The respective Arrhenius plot is shown in Fig. 4A and it yielded an activation energy of 77 kJ/mol.

Leaching of sphalerite. Virtually complete solubilization of zinc was achieved at >16°C test temperatures (Fig. 5A). The rate of leaching was proportional to the residual zinc concentration (Fig. 5B), thereby representing an example of the shrinking particle model. The effect of temperature was particularly noticeable on the length of the lag period preceding the active leaching.

The kinetic parameters are summarized in Table 2. The rate constants yielded a linear Arrhenius plot (Fig. 4B) and an activation energy value of 45 kJ/mol.

Leaching of pyrrhotite. The bacterial leaching of nickel at each test temperature is shown in Fig. 6A. Nickel was distributed in both the pentlandite and pyrrhotite phases, with a minor amount in pyrite. Based on their relative abundance and Ni content, it was estimated that approximately 50% of the total Ni was in pyrrhotite. We have found that the leaching rate of pyrrhotite is higher than that of pentlandite or pyrite; this difference is also in good agreement with mineralogical investigations of leach residues (unpublished results). Thus, the initial dissolution of nickel was taken to represent the leaching of pyrrhotite in the present work.

The pattern of nickel leaching displayed an initially fast phase followed by a second, declining phase. The data were found to fit a straight-line relationship in a parabolic plot (Fig. 6B). This is representative of a shrinking core model which assumes that the rate of leaching is inversely proportional to the concentration of the dissolved metal. The respective kinetic parameters are listed in Table 3. The rate constants derived with the parabolic model displayed linearity in the Arrhenius plot (Fig. 4C) and yielded an activation energy value of 40 kJ/mol.

Leaching of pyrite. Pyrite leaching was evaluated indirectly based on the dissolution of cobalt and on the decrease in pH. Based on the relative abundance of pyrite and pentlandite and their Co content, it was estimated that approximately two-thirds of the total Co was associated with pyrite. The leaching of cobalt at the test temperatures is shown in Fig. 7A. The profile of cobalt leaching indicated linearity and did not resemble the same parabolic type of time course that was observed for nickel.

The soluble cobalt is related to the leaching of both pyrite and pentlandite. The molar ratio of Co/(Co + Ni) for each temperature is shown in Fig. 8. The increases in the ratios of Co/(Co + Ni) shown in Fig. 8 demonstrate preferential pyrite oxidation. A constant ratio would indicate (i) preferential pentlandite oxidation or (ii) the simultaneous oxidation of both pyrite and pyrrhotite. Decreasing ratios would indicate pyrrhotite dissolution.

Figure 7B demonstrates the temperature relationship of cobalt dissolution, and this is considered to represent mainly pyrite oxidation. The kinetic parameters of pyrite oxidation are summarized in Table 4. An activation energy value of 95.5 kJ/mol was estimated from the respective Arrhenius plot shown in Fig. 4D. Of the minerals examined in this study, the bacterial leaching of pyrite displayed the highest temperature dependence, as is also apparent from the high E_a value.

Chemical leaching rates. The rate constants for each mineral in the uninoculated control flasks were calculated in the same way as for the respective inoculated experiments. A ratio of the rate constants of the chemical and bacterial leaching ($k_{bacterial}/k_{chemical}$) is shown in Fig. 9. The ratio was highest (about 12 to 15) for sphalerite. For chalcopyrite and pyrrhotite, the ratios were in the range of 5 to 9 and 2 to 4, respectively. These ratios were relatively independent of the test temperature. However, a strong temperature dependence was apparent with cobalt, for which the ratio increased from about 1 at 4°C to 17 at 37°C. These ratios for cobalt primarily represent the relative differences between the bacterial and chemical leaching of pyrite.

DISCUSSION

To our knowledge, this study is the first to report activation energy values for bacterial leaching of several minerals

in one ore material. The values were different for the sulfide minerals examined. The relatively high activation energy values for chalcopyrite and pyrite indicated the existence of a chemical or biochemical control of the leaching process. This control is mineral specific as otherwise the respective activation energy values would be the same for each mineral. The rate-determining step can also be a mineral-specific chemical reaction, as, for example, the initial release of the metal ion from the mineral lattice.

The relatively low E_a values for pyrrhotite and sphalerite suggest a mixed control due to diffusion as well as a chemical or biochemical reaction. Galvanic coupling effects between sphalerite-pyrite or sphalerite-chalcopyrite may decrease the kinetic barriers of sphalerite oxidation. Thus, galvanic effects may emphasize the role of movement of metal ions in the vicinity of mineral surface as the rate-determining steps. In general, rate-controlling phenomena in bacterial leaching systems are poorly understood, and available experimental information on rate-limiting steps in these complex processes is insufficient to evaluate the actual mechanisms. To date, mathematical models have not been developed for dynamic interactions, such as those described in the present study between pH, redox potential, temperature, and bacterial activity toward chalcopyrite solubilization, common in bacterial leaching processes.

For chalcopyrite, the leaching of copper was initially fast but subsequently declined to more or less constant rates. The temperature dependence of chalcopyrite oxidation was partially masked by changes in pH and redox potential. Parabolic kinetics due to the formation of product zone have been reported previously for chalcopyrite (4). In the present work, the k values were estimated from those parts of the time courses which displayed apparent steady states as defined by comparable rates of formation and removal of the product zone.

A comparison of the bacterial and chemical leaching rates demonstrates that the bacterial catalytic effect is most pronounced for sphalerite and pyrite. The bacterial catalysis of cobalt leaching was distinctly temperature dependent. A possible explanation for this observation is that the rate-determining step is different for the bacterial and chemical oxidation of pyrite, whereas the rate-determining steps in the leaching of the other sulfide minerals do not discriminate between the bacterial and chemical reactions.

ACKNOWLEDGMENTS

Partial funding for this work was received from the Ministry of Trade and Industry (Finland), Outokumpu Ltd., and the Nordisk Industrifond.

We thank Petteri Hietanen for skillful technical assistance, Outokumpu Ltd. for ore samples and metal analyses, and Laurie Haldeman for typing the manuscript.

REFERENCES

1. **Ahonen, L., and O. H. Tuovinen.** 1989. Microbiological oxidation of ferrous iron at low temperatures. Appl. Environ. Microbiol. **55:**312–316.
2. **Ahonen, L., and O. H. Tuovinen.** 1990. Kinetics of sulfur oxidation at suboptimal temperatures. Appl. Environ. Microbiol. **56:** 560–562.
3. **Blancarte-Zurita, M. A., R. M. R. Branion, and R. W. Lawrence.** 1986. Application of a shrinking particle model to the kinetics of microbiological leaching, p. 243–253. *In* R. W. Lawrence, R. M. R. Branion, and H. G. Ebner (ed.), Fundamental and applied biohydrometallurgy. Elsevier Science Publishers, Amsterdam.
4. **Dutrizac, J. E., and R. J. MacDonald.** 1974. Ferric ion as a leaching medium. Miner. Sci. Eng. **6:**59–100.
5. **Sohn, H. Y.** 1979. Fundamentals of the kinetics of heterogeneous reaction systems, p. 1–42. *In* H. Y. Sohn and M. E. Wadsworth (ed.), Rate processes of extractive metallurgy. Plenum Press, New York.
6. **Wadsworth, M. E.** 1979. Hydrometallurgical processes, p. 133–241. *In* H. Y. Sohn and M. E. Wadsworth (ed.), Rate processes of extractive metallurgy. Plenum Press, New York.